# Controlled fabrication of polymer microgels by polymer-analogous gelation in droplet microfluidics†

**Sebastian Seiffert and David A. Weitz**

***Received 7th March 2010, Accepted 29th April 2010***
***First published as an Advance Article on the web 21st May 2010***
**DOI: 10.1039/c0sm00071j**

We fabricate thermo-responsive polymer microgels by combining microfluidic pre-gel emulsification with polymer-analogous gelation. This separates the microgel formation from the polymer synthesis; it combines highly controlled microfluidic templating with the great flexibility of preparative polymer chemistry, allowing each to be controlled independently. We produce monodisperse pre-gel droplets from semidilute solutions of photocrosslinkable poly(*N*-isopropylacrylamide) precursors. The size and morphology of these droplets can be precisely controlled by the microfluidic emulsification, provided the molecular weight of the precursor is limited. Using polymer-analogous gelation rather than monomer chain-growth gelation yields gels with a higher efficiency of crosslinking and a greater homogeneity on nano- and micrometre scales, as determined by oscillatory shear rheology, static light scattering, and optical microscopy. We also demonstrate the applicability of our method to fabricate microgel particles with well-defined concentrations of functional sites.

## Introduction

Polymer microparticles which exhibit a tunable swelling and shrinking behavior are often referred to as stimuli-sensitive or "smart" microgels; they are fascinating materials with great potential for a variety of applications.[1–3] An elegant method to fabricate such microgels in the challenging size range of 10–1000 μm is through the use of droplet microfluidics,[4–11] which produces highly monodisperse particles of well-controlled size and morphology.[6,8,9,11,12–16] This method has been used extensively to prepare environmentally sensitive microgels, primarily comprised of poly(*N*-isopropylacrylamide) (pNIPAAm).[8,9,11,14,16] In all cases, a crude gelation scheme was employed; the monomer, *N*-isopropylacrylamide (NIPAAm), was reacted with a crosslinker, typically *N*,*N*′-methylenebiscarylamide (BIS), in a free-radical crosslinking copolymerization. This strategy has some intrinsic limitations: first, the resultant polymer networks are inhomogeneous on a nanoscale; this is commonly attributed to strong spatial concentration fluctuations during the early phase of the polymerization.[17–19] Moreover, these hydrogels often exhibit inhomogeneities on micron length scales, stemming from microphase separation during the sol–gel transition due to the pronounced heat of polymerization.[20,21] Second, when microgels are produced by copolymerizing monomers and crosslinkers, their total degree of polymerization and crosslinking is not well defined; moreover, when multiple functionalities are incorporated, their very composition and chain architecture are also not well defined. Indeed, the concentration of monomer, crosslinker, and, where appropriate, additional comonomers can be controlled only *prior* to polymerization; the efficiency and uniformity of the subsequent polymerization cannot be controlled, and can often even not be determined. These drawbacks limit the utility of pNIPAAm microgels: network inhomogeneities are undesirable for fundamental studies of microgel properties; moreover, they are detrimental for encapsulation applications. In addition, the poor control over composition and chain architecture limits flexibility in producing highly functional, custom-made microgels for advanced sensing or actuation purposes.

Instead of using monomer solutions, an excellent strategy to circumvent these drawbacks is to form the drops with semidilute solutions of pre-fabricated precursor polymers, and to crosslink these in a polymer-analogous reaction; this separates the particle formation from the material synthesis. A very similar approach has successfully produced crosslinked alginate or gelatin microparticles.[3,22–27] However, this approach has never been adopted to prepare functional pNIPAAm microgels.

In this paper, we use microfluidic devices to produce monodisperse pNIPAAm microgels using a polymer-analogous crosslinking reaction. We fabricate thermo-responsive particles by emulsifying semidilute solutions of functional pNIPAAm precursors and crosslinking the chains in the dispersed phase through a photochemical pathway, as sketched in Fig. 1A. We show that this method leads to gels with higher crosslinking efficiency and greater homogeneity on the nano- and micron-scale than does the classical free-radical crosslinking copolymerization technique. We also illustrate the utility of our strategy to form pNIPAAm particles with well-defined amounts of additional functional sites.

## Results and discussion

To realize our concept, we use linear pNIPAAm chains with pendant dimethylmaleimide (DMMI) side groups as precursor polymers. The DMMI moieties can be transformed into dimers upon UV exposure in the presence of a triplet sensitizer such as

*Harvard University, School of Engineering and Applied Sciences and Department of Physics, 29 Oxford Street, Cambridge, MA, 02138, USA. E-mail: seiffert@seas.harvard.edu; weitz@seas.harvard.edu*

† Electronic supplementary information (ESI) available: Full experimental details. See DOI: 10.1039/c0sm00071j

 

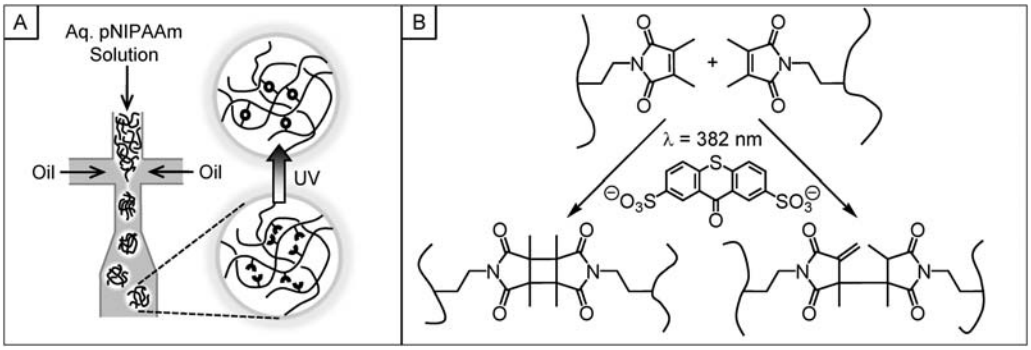


**Fig. 1** Schematic of a polymer-analogous gelation to form microgels with droplet microfluidics. (A) Sketch of a microfluidic device emulsifying a semidilute poly(*N*-isopropylacrylamide) (pNIPAAm) solution in water. Subsequent crosslinking of the chains by dimerizing reactive side groups with a photochemical reaction forms polymer microgels. (B) UV-induced crosslinking of dimethylmaleimide (DMMI) functionalized polymers. In aqueous media, the reaction is mediated by a triplet sensitizer, thioxanthone-2,7-disulfonate. Two isomeric types of DMMI-dimers are formed, each constituting a covalent junction between the precursor chains.[28,29]

thioxanthone disulfonate (TXS), leading to a permanent chain interconnection as sketched in Fig. 1B.[28,29] DMMI has only a small influence on the thermo-responsiveness of pNIPAAm.[30–35] Moreover, the transformation of DMMI moieties into dimers can be gradual,[36] and the progress of the reaction can be monitored by UV spectroscopy.[28]

We prepare our photocrosslinkable precursors by copolymerizing *N*-isopropylacrylamide and a DMMI-functionalized acrylamide-derivative in a free-radical reaction in water, as illustrated in Fig. 2A. To control the molecular weight of the products, we perform this polymerization in the presence of sodium formate which acts as a chain transfer agent in aqueous media.[37–39] We check for the impact of this additive by measuring the molecular weight distributions of eight samples polymerized with different concentrations of sodium formate, yielding weight average molecular weights between 135 000 g mol$^{-1}$ (high content of sodium formate) and 1 700 000 g mol$^{-1}$ (no sodium formate), as detailed in Fig. 2B. The presence of sodium formate also reduces the width of the molecular weight distributions. In the present experimental series, the polydispersity index, $M_w/M_n$, varies from 2.0 to 5.6.

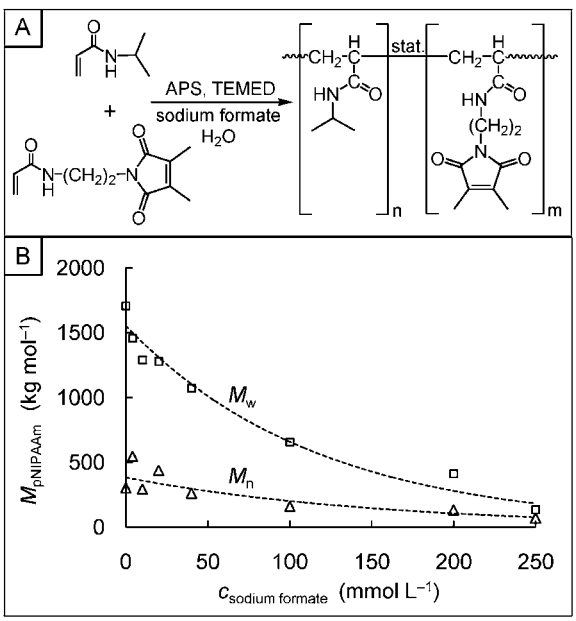


**Fig. 2** Preparation and molecular weight control of photocrosslinkable poly(*N*-isopropylacrylamide) (pNIPAAm). (A) Schematic of the copolymerization of *N*-isopropylacrylamide (NIPAAm) and DMMI-functionalized acrylamide (DMMIAAm). (B) Number ($M_n$) and weight ($M_w$) average molecular weight of pNIPAAm as polymerized through an aqueous free-radical polymerization in the presence of different concentrations of sodium formate. All samples were polymerized at total monomer concentrations of 0.25 mol L$^{-1}$, and all reactions were triggered by ammonium persulfate (APS) and *N*,*N*,*N*′,*N*′-tetramethylethylenediamine (TEMED). Finally, each reaction was interrupted at low conversion (~10%), and the products were characterized by size exclusion chromatography. The dotted lines are guides to the eye.

To create pre-gel droplets of our precursors, we use solutions with concentrations in the semidilute unentangled regime, an intermediate range right above the threshold for coil overlap, $c^*$, yet below the onset of chain entanglement, $c_e^*$.[40–42] Using a concentration above $c^*$ ensures that a space-filling polymer network can be formed within each droplet, whereas using a concentration below $c_e^*$ ensures that the viscosity of the solution is not too high. To check whether polymer solutions in this regime can be emulsified in a controlled fashion, we conduct microfluidic experiments with four different aqueous pNIPAAm solutions. These solutions explore different molecular weights and concentrations between $c^*$ and $c_e^*$, as detailed in Table 1. The continuous phase in all these experiments is a highly viscous paraffin oil ($\eta$(1 rad s$^{-1}$) = 130 mPa s) containing 2 wt% of a modified polyether–polysiloxane surfactant (ABIL EM 90, Evonik Industries, Germany). We emulsify our polymer solutions using a flow focusing glass capillary microfluidic device[8,9] and probe the behavior at different ratios of the flow rates of the inner (aqueous) and outer (oil) fluids, $Q_{aq}/Q_{oil}$, by monitoring the flow-patterns as illustrated in Fig. 3.

We find that semidilute solutions of comparably *short* chains can be easily emulsified to form monodisperse droplets. We observe controlled dripping for samples that consist of low molecular weight pNIPAAm ($M_w$ = 410 000 g mol$^{-1}$) with concentrations spanning the range between 2$c^*$ and 10$c^*$ (System I, left part of Fig. 3). Adjusting $Q_{aq}/Q_{oil}$ controls the size of the drops over a wide range. Similar behavior is also observed at slightly higher molecular weight ($M_w$ = 660 000 g mol$^{-1}$) and

**Table 1** Material properties of four different semidilute pNIPAAm solutions used to study their ability to be emulsified in microfluidic devices, as shown in Fig. 3. $M_n$ denotes the number average molecular weight, whereas $M_w$ is the weight average molecular weight. $[\eta]$ is the intrinsic viscosity as estimated by aqueous solution viscometry ($T = 20$ °C, Ubbelohde viscometer). From this quantity, the overlap concentration, $c^*$, can be calculated as $c^* = 1/[\eta]$.[42] We choose the concentration of the polymer, $c$, in our four systems such to explore different ranges in the interval 2–10$c^*$. $\eta$ denotes the dynamic viscosity as obtained by shear viscometry at a rate of 1 rad s$^{-1}$ ($T = 25$ °C, Anton Paar G2 rheometer, cone–plate geometry)

| System No. | $M_n$/g mol$^{-1}$ | $M_w$/g mol$^{-1}$ | $[\eta]$/mL g$^{-1}$ | $c^* \approx 1/[\eta]$/g L$^{-1}$ | $c$/g L$^{-1}$ | $c$/rel. to $c^*$ | $\eta$(1 rad s$^{-1}$)/mPa s |
|---|---|---|---|---|---|---|---|
| I | 130 000 | 410 000 | 92 | 11 | 20–100 | 2–10$c^*$ | 27–130 |
| II | 160 000 | 660 000 | 152 | 7 | 20 | 3$c^*$ | 65 |
| III | 160 000 | 660 000 | 152 | 7 | 50 | 7$c^*$ | 84 |
| IV | 550 000 | 1 460 000 | 327 | 3 | 10–20 | 3–7$c^*$ | 40–90 |

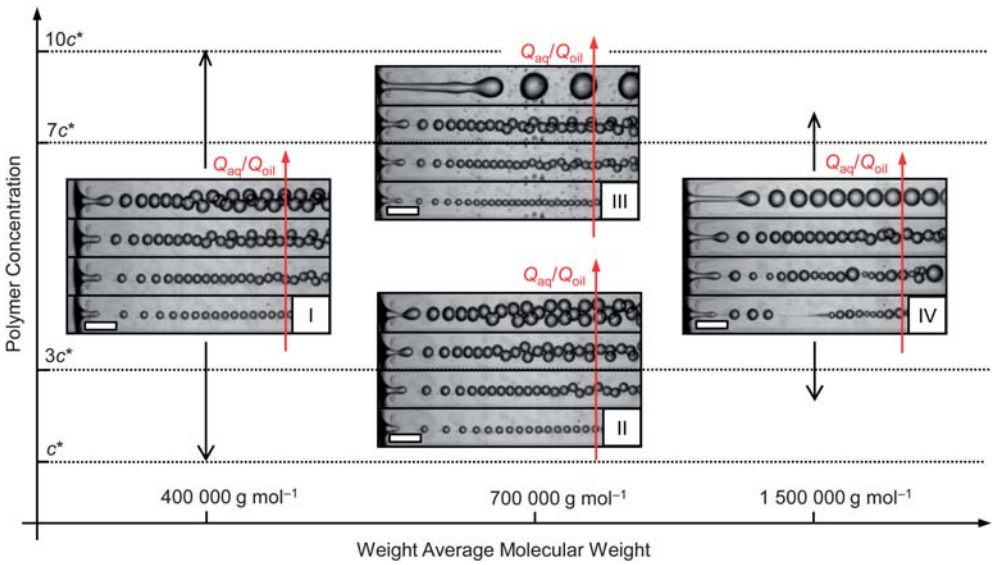


**Fig. 3** Droplet formation of semidilute poly(*N*-isopropylacrylamide) solutions in a glass capillary microfluidic device as a function of polymer concentration, molecular weight, and flow rates of the fluids. The micrographs show characteristic results observed for four different samples in the semidilute regime (labeled by Roman numerals I–IV), the compositions of which are detailed in Table 1. Each sample was probed at four different ratios between the flow rate of the polymer phase, $Q_{aq}$, and the flow rate of the continuous phase, $Q_{oil}$, respectively. The ratio $Q_{aq}/Q_{oil}$ increases from the lowermost to the uppermost picture within each stack of images (*cf.* ESI†). All scale bars denote 500 μm.

a concentration of 3$c^*$ (System II, lower middle part of Fig. 3). By contrast, at a higher concentration of 7$c^*$, monodisperse drops are formed only over a limited range of flow rates, with less controlled jetting occurring at higher $Q_{aq}/Q_{oil}$ (System III, upper middle part of Fig. 3). If the chain molecular weight is very high ($M_w$ = 1 460 000 g mol$^{-1}$, System IV), monodisperse drops are obtained only for a narrow range of $Q_{aq}/Q_{oil}$; lower values lead to unstable drop formation, whereas higher values lead to less controlled jetting. These results are observed at both low concentrations, 3$c^*$, and higher concentrations, 7$c^*$, as depicted in the right part of Fig. 3.

After creating pre-gel droplets, microgel particles are obtained by crosslinking the precursor chains inside them. This is accomplished using a suitable microfluidic device which allows exposure of the droplets to UV immediately after their formation; this avoids transport of the drops through long channels, where they can coalesce or split if they are not yet gelled. We use soft lithography to fabricate a microfluidic device from polydimethylsiloxane (PDMS)[43] and create droplets with diameters of about 60 μm using a cross-junction geometry,[5] as shown in Fig. 4A. These drops contain a 50 g L$^{-1}$ precursor solution of a crosslinkable pNIPAAm ($M_w$ = 200 000 g mol$^{-1}$, DMMI content 0.75 mol%). To sensitize the crosslinking reaction, we add 0.5 mmol L$^{-1}$ TXS to the aqueous phase. This concentration of photosensitizer results in a transmittance of about 97% in the range of its absorption maximum ($\lambda$ = 382 nm, $\epsilon$ = 4540 L mol$^{-1}$ cm$^{-1}$) over a distance of 60 μm; this avoids the build-up of a gradient of crosslink density across the particles. The monodisperse pre-gel drops are exposed to strong UV light ($\lambda$ = 300–500 nm, intensity about 250 mW cm$^{-2}$) about three centimetres downstream to crosslink the polymer and thus solidify the drops. The resultant monodisperse microgel particles are shown in Fig. 4B. Similar microgel particles, but with diameters of about 150 μm obtained from a device with a larger channel, are shown in Fig. 4C.

In addition to formulating simple spherical microgels, we also fabricate micro*shells* from double emulsion templates.[8,9] In a typical experiment, we use a glass microcapillary device to create drops of the same semidilute pNIPAAm precursor solution. The continuous phase in this experiment is again paraffin oil containing 2 wt% ABIL EM 90, and the aqueous droplets contain inner droplets of kerosene plus the same surfactant, thereby creating a shell structure. A typical device for fabricating these core–shell double emulsions is shown in Fig. 4D. After their

 

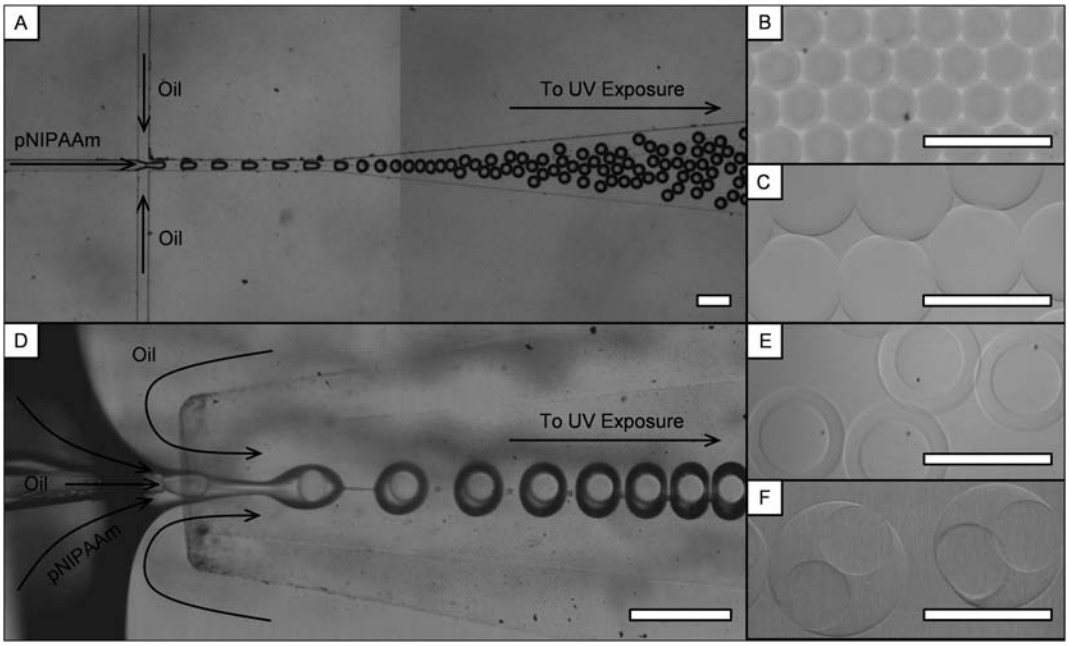


**Fig. 4** Formation of pNIPAAm microparticles from semidilute precursor solutions. (A) Production of monodisperse pNIPAAm microgels in a PDMS microfluidic device. A cross-junction produces monodisperse pre-gel droplets, which are exposed to strong UV light a few centimetres downstream within the same channel to solidify them. (B) Monodisperse microgels obtained from the experiment shown in panel A. (C) Larger microgels as obtained from a similar experiment using a bigger microchannel geometry. (D) Production of an oil-water-oil double emulsion with a semidilute pNIPAAm solution as aqueous phase using a glass capillary microfluidic device. Similar to the experiment in panel A, the droplets are cured in a delay capillary a few centimetres downstream (not shown). (E) pNIPAAm microshells obtained from the experiment shown in panel D. (F) Double-core microshells as obtained upon slight variation of the flow rates in the experiment shown in panel D. All scale bars denote 200 μm.

formation, the shell is gelled by exposure to UV light ($\lambda$ = 365 nm, intensity about 20 mW cm$^{-2}$) while flowing through a delay-line capillary. This yields the uniform pNIPAAm microshells shown in Fig. 4E. Operating the device with different flow rates (ESI†) produces shells with two cores, as shown in Fig. 4F.

To demonstrate the gelation efficiency of our polymer-analogous approach, we measure the shear modulus of macroscopic gel samples, enabling us to determine their crosslink density using the theory of rubber elasticity. We use samples gelled from a pNIPAAm precursor with a DMMI-content of 3 mol%, which

**Table 2** Rheological and static light scattering characterization of semidilute bulk hydrogels obtained through a chain-growth gelation or a polymer-analogous gelation. (A) Elastic ($G'$) and viscous ($G''$) part of the complex shear modulus as measured by oscillatory shear rheology, as well as concentration of junctions ($\nu$) calculated from the formula $G' \approx G = \nu RT$ derived from the theory of rubber elasticity with the assumption of fluctuating junctions ($T = 25$ °C, $R = 8.31$ J K$^{-1}$ mol$^{-1}$). The ratio of $\nu$ and its theoretical value, $\nu_{theo}$, as calculated from the molar concentration of crosslinkers or crosslinkable groups in the samples, provides an estimate of the efficiency of crosslinking. (B) Elastic moduli ($G'$) and crosslinking efficiencies ($\nu/\nu_{theo}$) as obtained by oscillatory shear rheology, as well as relative root-mean-square concentration fluctuations ($\langle\delta c^2\rangle^{1/2}$) as obtained by static light scattering experiments followed by data evaluation with the Debye–Bueche method

(A)

| Photochemical polymer-analogous gelation | | | | | | Free-radical chain-growth gelation | | | | | |
|---|---|---|---|---|---|---|---|---|---|---|---|
| $c_{total}$/g L$^{-1}$ | $c_{DMMI}$ (mol%) | $G'$/Pa | $G''$/Pa | $\nu$/mmol L$^{-1}$ | $\nu/\nu_{theo}$ (%) | $c_{total}$/g L$^{-1}$ | $c_{BIS}$ (mol%) | $G'$/Pa | $G''$/Pa | $\nu$/mmol L$^{-1}$ | $\nu/\nu_{theo}$ (%) |
| 20 | 3 | 90 | 5 | 0.035 | 1.4 | 20 | 1.5 | No gelation | | | |
| 50 | 3 | 3320 | 110 | 1.342 | 20.8 | 50 | 1.5 | 670 | 11 | 0.272 | 4.1 |
| 100 | 3 | 11000 | 1420 | 4.416 | 34.3 | 100 | 1.5 | 5960 | 215 | 2.396 | 18.1 |

(B)

| Photochemical polymer-analogous gelation | | | | | Free-radical chain-growth gelation | | | | |
|---|---|---|---|---|---|---|---|---|---|
| $c_{total}$/g L$^{-1}$ | $c_{DMMI}$ (mol%) | $G'$/Pa | $\nu/\nu_{theo}$ (%) | $\langle\delta c^2\rangle^{1/2}$ (%) | $c_{total}$/g L$^{-1}$ | $c_{BIS}$ (mol%) | $G'$/Pa | $\nu/\nu_{theo}$ (%) | $\langle\delta c^2\rangle^{1/2}$ (%) |
| 25 | 0.75 | 70 | 3.5 | 29 | 25 | No gelation | | | |
| 50 | 0.75 | 925 | 22.7 | 15 | 50 | 1.30 | 934 | 6.6 | 44 |
| 100 | 0.75 | 3310 | 40.6 | 6 | 100 | 0.65 | 3300 | 23.1 | 57 |

corresponds to a theoretical crosslink density of 1.5 mol%. Semidilute aqueous solutions ($c = 20$–$100$ g L$^{-1}$) of this material were cured on a rheometer equipped with a plate–plate geometry, and oscillatory shear measurements were conducted at temperatures around $T = 25$ °C. For all these samples, the storage modulus, $G'$, exhibits a frequency-independent plateau at low frequencies, enabling us to determine the elasticity of the gels. With these values, we estimate the molar concentration of junctions, $\nu$, using the simple relation $G' \approx G = \nu RT$ derived from the phantom network model,[40,42,44–46] which is commonly applied to gels in the semidilute regime[17] ($R = 8.31$ J K$^{-1}$ mol$^{-1}$). If all DMMI-moieties formed crosslinks, the concentration of junctions would be $\nu_{\text{theo}}$; thus, $\nu/\nu_{\text{theo}}$ provides an estimate of the efficiency of crosslinking. For our photogelled samples, $\nu/\nu_{\text{theo}}$ rises from 1.4% in a 20 g L$^{-1}$ system to 34% in a 100 g L$^{-1}$ system. By contrast, crosslinking is less efficient in samples gelled by a chain-growth process; gels formed by copolymerizing NIPAAm and BIS in a free-radical reaction exhibit efficiencies of only 4% and 18% in a 50 and 100 g L$^{-1}$ system, while there is no gelation at all in a 20 g L$^{-1}$ system, as summarized in Table 2A. Thus, polymer-analogous gelation is superior, requiring much less material than the chain-growth process to form gels with comparable elastic properties; it also allows gels to be made at low concentrations at which the chain-growth reaction does not gel at all.

To appraise the nanoscale homogeneity of our gels, we estimate their percentage root-mean-square concentration fluctuation (Table 2B); this is done with static light scattering. Generally, the scattering intensity of a gel can be assumed to be the sum of thermal concentration fluctuations (ergodic contribution) and of static spatial inhomogeneities resulting from the crosslinking process (nonergodic contribution). To determine the latter quantity, one may presume that the thermal fluctuations are identical to those in an uncrosslinked semidilute solution of the same polymer. Hence, the excess scattering intensity of a polymer gel can be determined from the difference of the angle-resolved scattering between a crosslinked and an uncrosslinked sample.[19] Subsequent data evaluation by the Debye–Bueche method yields two characteristic network parameters: the static correlation length and the root-mean-square refractive index fluctuation, which can be converted into concentration fluctuations if the refractive index increment is known.[17,18]

We perform these analyses on bulk samples gelled from a precursor polymer with $M_w = 200\,000$ g mol$^{-1}$ and a DMMI-content of 0.75 mol%, which corresponds to $\nu_{\text{theo}} = 0.375$ mol%, and find that the relative concentration fluctuations in these networks decrease from 29% to only 6% as the concentration increases from 25 to 100 g L$^{-1}$ (Table 2B, column 5; *cf.* ESI† for experimental details and data evaluation). Concurrently, the elastic modulus and efficiency of crosslinking increase, as measured by shear rheology (column 3 and 4). By contrast, we observe strong inhomogeneities in gels formed through a free-radical crosslinking copolymerization of NIPAAm and BIS. If we prepare a set of samples such that they show very similar elastic moduli as their photogelled counterparts, we need to use much more BIS than DMMI (column 2 and 7), which leads to gels with pronounced nanoscale inhomogeneities: while there is no gelation in a 25 g L$^{-1}$ system, samples with concentrations of 50 and 100 g L$^{-1}$ show relative root-mean-square concentration fluctuations of around 50% (column 10).

These results can be explained by considering the gelation mechanism. In the early phase of a free-radical crosslinking copolymerization, extensive cyclization and multiple crosslinking reactions take place, leading to an assembly of spatially localized nanogels. As the reaction proceeds to higher conversion, macroscopic gelation occurs by interconnecting these clusters to a continuous network. Hence, the resulting space-filling gel is an irregular assembly of nanogel clusters tied loosely together, leading to pronounced concentration fluctuations on a length scale of several ten nanometres.[17–19] By contrast, interconnecting pre-fabricated chains in a semidilute solution just locks the homogeneous structure of the physically entangled pre-gel network.

In addition to their inhomogeneities on a nanoscale, pNIPAAm networks often show pronounced *micron*-scale inhomogeneities. These can be induced if the gelation process is fast and occurs with a marked evolution of heat; local increase of the temperature above the lower critical solution temperature of pNIPAAm causes microphase separation which leads to microporous gels.[20,21] To check whether this impairs the fabrication of

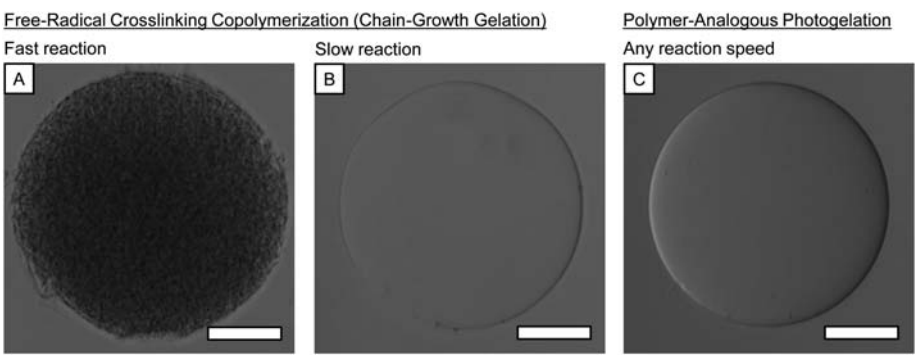


**Fig. 5** Micrographs of pNIPAAm microgels formed by free-radical crosslinking copolymerization (A and B) or by selectively crosslinking pre-polymerized precursor chains (C). The gelation of the particle in panel A occurred within a few seconds, resulting in marked micron-scale inhomogeneities. By contrast, the formation of the particle in panel B took several hours and no micron-scale inhomogeneities are observed. The particle obtained from the photochemical polymer-analogous gelation (panel C) was gelled in just a few seconds without marked impact on its optical appearance on a micron-scale. All scale bars denote 50 μm.

 

pNIPAAm microgels from pre-gel emulsions, we compare optical micrographs of particles prepared by three different reactions. First, we consider free-radically gelled microgels with a total concentration of 150 g $L^{-1}$ and a degree of BIS of 1.5 mol%. If we trigger their polymerization by adding 3 mol% of ammonium persulfate (APS) to the aqueous and 10 vol% of *N*,*N*,*N*′,*N*′-tetramethylethylenediamine (TEMED) to the continuous phase, we form microgels through a very rapid reaction. These particles exhibit pronounced inhomogeneities on a micrometre length scale, as shown in Fig. 5A. By contrast, gelling these microgels with only 0.75 mol% APS in the aqueous and 1 vol% TEMED in the continuous phase yields homogeneous microstructures, as shown in Fig. 5B. However, this homogeneity is achieved only using reaction times of several hours at room temperature.

Microgels formed using the polymer-analogous photogelation do not exhibit any micron-scale heterogeneities, as exemplified in Fig. 5C for a particle gelled from a 50 g $L^{-1}$ solution of a precursor polymer with a DMMI-content of 3 mol%. Even though this particle was gelled in just a few seconds (TXS concentration 0.5 mmol $L^{-1}$, UV intensity about 250 mW $cm^{-2}$, $\lambda = 300$–500 nm), its gelation was not accompanied by microphase separation, because the TXS-sensitized DMMI-dimerization does not occur with a pronounced evolution of heat. Thus, this method is very useful when pre-gel droplets must be gelled quickly yet homogeneously.

The polymer-analogous microgel production provides another useful benefit: it separates particle formation from the polymer synthesis, allowing microgels to be fabricated from highly *pre-functionalized* materials which provide well-defined amounts of arbitrary functionalities. One strategy to impart many different functional sites into microgels is to use several different precursor polymers, each imparting its own functionality. These precursors need only to be terpolymers which contain a main monomer, a crosslinkable comonomer, and another functional comonomer. Mixing several of such terpolymers allows us to produce particles with a precisely defined composition and degree of functionalization.

To demonstrate this concept, we prepare pNIPAAm particles which contain precisely defined amounts of different fluorescent dyes, representing arbitrary functional sites. These dyes are easy to detect, and their concentration in the microgel particles can be precisely quantified. We use mixtures of an unlabeled crosslinkable matrix material which is doped with well-defined amounts of red- and green-tagged crosslinkable pNIPAAm chains and cure them by our photogelation method, as sketched in Fig. 6A. Our tagged precursors contain 0.1 mol% of either Alexa Fluor 488 (Molecular Probes, Eugene, OR, USA) or carboxyrhodamine (Sigma Aldrich); they also contain 1 mol% of crosslinkable DMMI-moieties. We prepare four different samples consisting of a matrix material of 35 g $L^{-1}$ unlabeled photocrosslinkable pNIPAAm plus red- and green-tagged material in quantities of 15 and 0, 10 and 5, 5 and 10, or 0 and 15 g $L^{-1}$.

After emulsifying these solutions in a microfluidic device and photogelling the aqueous droplets, we obtain monodisperse particles which contain the same fractions of red and green dye as their corresponding precursor mixtures. To prove this, we image the resulting particle suspensions with a confocal laser scanning fluorescence microscope (Leica TCS SP5). We use either the

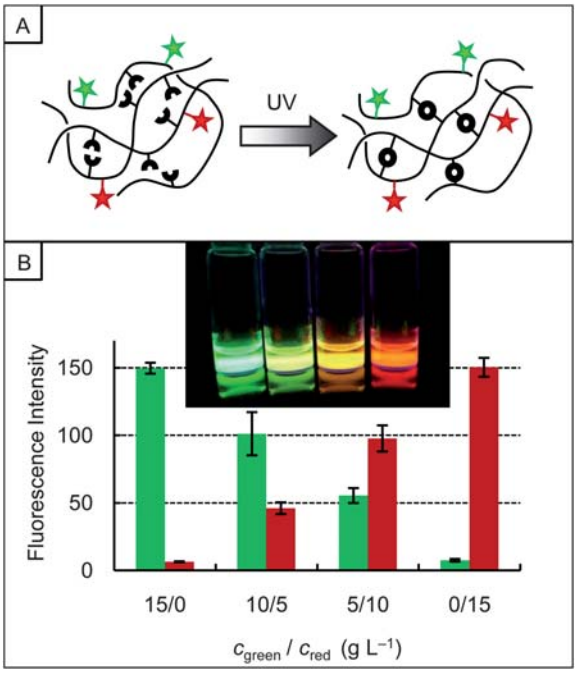


**Fig. 6** Production of highly functional microgels. (A) Schematic of a polymer-analogous crosslinking procedure using red- and green-tagged precursors. (B) Average fluorescence intensities of pNIPAAm microgels obtained from pre-gel mixtures which contain red- and green-labeled chains in concentrations as denoted on the abscissa. The fluorescence intensities were detected separately in a red (501–535 nm, red bars) and a green (558–638 nm, green bars) channel upon separate excitation of the dyes with a blue (488 nm) and a green laser (543 nm) line, respectively. The inset photograph shows the apparent fluorescence colors of the microgel samples.

488 nm line of an Ar ion laser or the 543 nm line of a HeNe laser to excite the two dyes independently. Fluorescence detection takes place in two separate channels in the range of 501–535 nm (green channel) and 558–638 nm (red channel), respectively. All laser powers and photomultiplier voltages are adjusted to obtain the same average fluorescence intensity in the red and the green detection channel when imaging microgels containing only 15 g $L^{-1}$ red- or only 15 g $L^{-1}$ green-dyed material; only a single color is excited and detected at any given time to avoid crosstalk between the two channels. The average fluorescence intensities of the four microgel samples detected with this method reflect the initial fractions of red and green dye in their respective pre-gel solutions within experimental error, as illustrated in Fig. 6B. Moreover, the fluorescence is distributed homogeneously across the particles.

## Conclusions

Homogeneous and well-defined microgel particles are advantageous for applications such as encapsulation and controlled release of actives. They are also useful when fundamental properties of microgels or their suspensions are studied. An advantage of our polymer-analogous photocrosslinking method is that this can be done with a *gradual* variation of the degree of crosslinking on the same sample by varying the photon fluence; this allows the

variation of this parameter to be studied with high precision. Moreover, our approach allows custom-made, highly functional, sensitive, or reactive microgels to be made. Depending on the monomer sequence in the precursor polymers, the spatial distribution of these functional sites across the microgel particles can be controlled on a nanometre scale. Thus, polymer-analogous gelation in droplet microfluidics offers promising means to fabricate new functional microgels for advanced sensing or actuation applications.

## Acknowledgements

We thank Julia Gansel, Saadet Dogu, and Markus Susoff (Clausthal University of Technology, Germany), who kindly provided the static light scattering data discussed in this paper and who performed part of the characterization of the precursor polymers used for this work. We also thank Rhutesh K. Shah and Changhyung Choi (Harvard University) for stimulating discussions and for their help with designing microfluidic devices. This work was supported by the NSF (DMR-0602684) and the Harvard MRSEC (DMR-0820484). SS received funding from the German Academy of Sciences Leopoldina (BMBF-LPD 9901/8-186), which is gratefully acknowledged.

## References

1 M. Ballauff, *Polymer*, 2007, **48**, 1815–1823.
2 M. Das, H. Zhang and E. Kumacheva, *Annu. Rev. Mater. Res.*, 2006, **36**, 117–142.
3 E. Tumarkin and E. Kumacheva, *Chem. Soc. Rev.*, 2009, **38**, 2161–2168.
4 S.-Y. Teh, R. Lin, L.-H. Hung and A. P. Lee, *Lab Chip*, 2008, **8**, 198–220.
5 S. L. Anna, N. Bontoux and H. A. Stone, *Appl. Phys. Lett.*, 2003, **82**, 364–366.
6 A. S. Utada, E. Lorenceau, D. R. Link, P. D. Kaplan, H. A. Stone and D. A. Weitz, *Science*, 2005, **308**, 537–541.
7 T. Nisisako, S. Okushima and T. Torii, *Soft Matter*, 2005, **1**, 23–27.
8 J.-W. Kim, A. S. Utada, A. Fernández-Nieves, Z. Hu and D. A. Weitz, *Angew. Chem., Int. Ed.*, 2007, **46**, 1819–1822.
9 L.-Y. Chu, A. S. Utada, R. K. Shah, J.-W. Kim and D. A. Weitz, *Angew. Chem., Int. Ed.*, 2007, **46**, 8970–8974.
10 M. Seo, C. Paquet, Z. Nie, S. Xu and E. Kumacheva, *Soft Matter*, 2007, **3**, 986–992.
11 R. K. Shah, H. C. Shum, A. C. Rowat, D. Lee, J. J. Agresti, A. S. Utada, L.-Y. Chu, J.-W. Kim, A. Fernandez-Nieves, C. J. Martinez and D. A. Weitz, *Mater. Today*, 2008, **11**, 18–27.
12 S. Xu, Z. Nie, M. Seo, P. C. Lewis and E. Kumacheva, *Angew. Chem., Int. Ed.*, 2005, **44**, 724–728.
13 Z. Nie, S. Xu, M. Seo, P. C. Lewis and E. Kumacheva, *J. Am. Chem. Soc.*, 2005, **127**, 8058–8063.
14 R. K. Shah, J.-W. Kim, J. J. Agresti, D. A. Weitz and L.-Y. Chu, *Soft Matter*, 2008, **4**, 2303–2323.
15 M. Seo, Z. Nie, S. Xu, M. Mok, P. C. Lewis, R. Graham and E. Kumacheva, *Langmuir*, 2005, **21**, 11614–11622.
16 F. Ikkai, S. Iwamoto, E. Adachi and M. Nakajima, *Colloid Polym. Sci.*, 2005, **283**, 1149–1153.
17 J. Nie, B. Du and W. Oppermann, *Macromolecules*, 2004, **37**, 6558–6564.
18 R. Liu and W. Oppermann, *Macromolecules*, 2006, **39**, 4159–4167.
19 M. Shibayama, *Bull. Chem. Soc. Jpn.*, 2006, **79**, 1799–1819.
20 C. Erbil, Y. Yildiz and N. Uyanik, *Polym. Int.*, 2000, **49**, 795–800.
21 C. Sayil and O. Okay, *Polymer*, 2001, **42**, 7639–7652.
22 S. Sugiura, T. Oda, Y. Izumida, Y. Aoyagi, M. Satake, A. Ochiai, N. Ohkohchi and M. Nakajama, *Biomaterials*, 2005, **26**, 3327–3331.
23 H. Zhang, E. Tumarkin, R. M. A. Sullan, G. C. Walker and E. Kumacheva, *Macromol. Rapid Commun.*, 2007, **28**, 527–538.
24 K.-S. Huang, T.-H. Lai and Y.-C. Lin, *Front. Biosci.*, 2007, **12**, 3061–3067.
25 C.-H. Yeh, Q. Zhao, S.-J. Lee and Y.-C. Lin, *Sens. Actuators, A*, 2009, **151**, 231–236.
26 K. Liu, H.-J. Ding, J. Liu, Y. Chen and X.-Z. Zhao, *Langmuir*, 2006, **22**, 9453–9457.
27 K.-S. Huang, K. Lu, C.-S. Yeh, R.-S. Chung, C.-H. Lin, C.-H. Yang and Y.-S. Dong, *J. Controlled Release*, 2009, **137**, 15–19.
28 S. Seiffert, W. Oppermann and K. Saalwaechter, *Polymer*, 2007, **48**, 5599–5611.
29 X. Yu, C. Corten, H. Goerner, T. Wolff and D. Kuckling, *J. Photochem. Photobiol., A*, 2008, **198**, 34–44.
30 L. Ling, W. D. Habicher, D. Kuckling and H.-J. P. Adler, *Des. Monomers Polym.*, 1999, **2**, 351–358.
31 D. Kuckling, H.-J. P. Adler, L. Ling, W. D. Habicher and F.-F. Arndt, *Polym. Bull.*, 2000, **44**, 269–276.
32 C. Duan Vo, D. Kuckling, H.-J. P. Adler and M. Schoenhoff, *Colloid Polym. Sci.*, 2002, **280**, 400–409.
33 D. Kuckling, C. Duan Vo and S. E. Wohlrab, *Langmuir*, 2002, **18**, 4263–4269.
34 D. Kuckling, J. Hoffmann, M. Plöttner, D. Ferse, K. Kretschmer, H.-J. P. Adler, K.-F. Arndt and R. Reichelt, *Polymer*, 2003, **44**, 4455–4462.
35 D. Kuckling, C. D. Vo, H.-J. P. Adler, A. Völkel and H. Cölfen, *Macromolecules*, 2006, **39**, 1585–1591.
36 S. Seiffert and W. Oppermann, *Polymer*, 2008, **49**, 4115–4126.
37 M. Pabon, J. Selb, F. Candau and R. G. Gilbert, *Polymer*, 1999, **40**, 3101–3106.
38 M. J. Fevola, R. D. Hester and C. L. McCormick, *J. Polym. Sci., Part A: Polym. Chem.*, 2003, **41**, 560–568.
39 S. Seiffert and W. Oppermann, *Macromol. Chem. Phys.*, 2007, **208**, 1744–1752.
40 M. Rubinstein, R. H. Colby, *Polymer Physics*, Oxford University Press, New York, 2003.
41 T. P. Lodge, N. A. Rotstein and S. Prager, *Adv. Chem. Phys.*, 1990, **79**, 1–132.
42 H. G. Elias, *Macromolecules; Vol. 3: Physical Structures and Properties*, Wiley VCH, Weinheim, 2008.
43 J. C. McDonald, D. C. Duffy, J. R. Anderson, D. T. Chiu, H. K. Wu, O. J. A. Schueller and G. M. Whitesides, *Electrophoresis*, 2000, **21**, 27–40.
44 H. James and E. Guth, *J. Chem. Phys.*, 1947, **15**, 669–683.
45 P. J. Flory, *Principles of Polymer Chemistry*, Cornell University Press, Ithaca, NY, 1953.
46 L. R. G. Treloar, *The Physics of Rubber Elasticity*, Clarendon Press, Oxford, 3rd edn, 1975.